Enhancement of Dye Sensitized Solar Cell Performance using Blocking Layer TiO_2 by Sputtering Method

Alfiatul Ma'arifah[1], Ikfa Rika Elma Suherlianti[1] dan Herlin Pujiarti[(1,2,a)*]

[(1)]Department of Physics, Faculty of Mathematics and Natural Sciences, Universitas Negeri Malang, Jl. Semarang No. 5, Malang, Indonesia, 65145
[(2)]Center of Advanced Materials and Renewable Energy, Universitas Negeri Malang, Jl. Semarang No. 5, Malang, Indonesia, 65145
Email : [(a)] herlin.pujiarti.fmipa@um.ac.id*

Disubmisi: 9 September 2025, Direvisi: 8 Desember 2025, Diterima; 5 Januari 2026

Abstract.
Background: *The efficiency of dye-sensitized solar cells (DSSC) can be improved through the use of a multilayer blocking layer (BL) of* TiO_2.
Aims: *In this study, the efficiency of dye-sensitized solar cells (DSSC) was improved through the use of a multilayer blocking layer (BL) of* TiO_2.
Methods: *Multilayer BL* TiO_2 *was deposited using a combination of sputtering and spin coating methods, which in previous studies were limited to using only one of these deposition methods.*
Results: *Based on the XRD results, the crystal size increased from 17.24 to 25.86 nm for multilayer BL* TiO_2. *Based on the SEM results, the morphology of all samples is quite uniform and suitable for the blocking layer, and the porosity of BL* TiO_2 *is smaller than that of multilayer BL* TiO_2. *Based on the UV-Vis absorbance results, the layer shifted from a wavelength of 248 to 257 nm, indicating a blue shift. The estimated energy gap decreased from 3.58 to 3.55 eV. Multilayer BL* TiO_2 *shows a high efficiency of 4.49% compared to BL* TiO_2 *with an efficiency of 2.50%. Additionally, based on the EIS results, the Rct decreased from 66.41 to 12.53 Ω.*
Conclusion: *These findings demonstrate that multilayer BL* TiO_2 *provides better photovoltaic performance than a single BL* TiO_2, *as evidenced by higher efficiency and lower Rct values.*

Keywords: *DSSC, multilayer blocking layer, spin coating, sputtering,* TiO_2.

PENDAHULUAN

Dye Sensitized Solar Cell (DSSC) is a third-generation photovoltaic device that converts sunlight into electrical energy [1]. DSSC was developed in 1991 by O'Regan and Gratzel [2]. DSSC is one of the third-generation solar cells with great potential for future applications [3]. This is due to its easy, affordable, flexible, environmentally friendly, and highly efficient production process [4], [5]. In general, DSSC is composed of a photoanode, electrolyte, dye, and counter electrode [6].

The photoanode itself consists of semiconductor nanoparticles placed on a transparent conductive glass that has been sensitized with a dye [7]. The most commonly used semiconductor layer is titanium dioxide (TiO_2), which has a band gap energy (E_g) of 3.20 eV [8]. In addition, TiO_2 has high porosity and surface area ratios, which allow for very intense contact with the sensitizing dye and greatly aid in the conversion of photons to electricity [8], [9].

It has been reported that charge recombination at the interface can significantly reduce photovoltaic performance [10]. In DSSC, charge recombination at the interface can be reduced by adding an blocking layer (BL) [11]. Adding a blocking layer (BL) creates a potential barrier between FTO and the semiconductor material, which can prevent electrons in FTO from returning to the semiconductor, thereby reducing recombination [12]. From the BL layer materials, TiO_2 shows the greatest potential to reduce back reaction, thereby increasing the short-circuit current (J_{sc}) of the DSSC device. This is because the TiO_2 BL layer can effectively enhance the adhesion of the photoanode to the TCO surface [13].

Although the BL can isolate the electrolyte from the electrode and effectively inhibit the recombination reaction between the electrode and the electrolyte, there are still a significant number of electrons that undergo back reaction and recombination with the electrolyte. Recently, multilayer BL has been introduced to reduce recombination and enhance charge transfer. In the multilayer BL, electrons can only flow from the electrolyte to the photoanode, which significantly inhibits the recombination reaction [14]. DSSC with a multilayer BL system shows an efficiency increase of up to 40% compared to BL [15]. The research conducted by Sibiński et al. using a multilayer BL Ti-Zn achieved an efficiency of 5.73% [16]. The research conducted by Ozel et al. using TiO_2/AZO achieved an efficiency of 5.77%. Whereas the TiO_2 BL alone produced an efficiency of 4.12% [15]. This improvement is associated with the reduction of charge recombination and the increase in J_{sc} [17]. Some of these studies are still limited to using only one single deposition technique, either sputtering or spin coating. However, research on the combination of both methods to fabricate multilayer BL TiO_2 is remains limited. Therefore, in this study, the performance of DSSC will be improved through multilayer BL TiO_2 using sputtering and spin coating methods.

MATERIALS AND METHODS

Material

The materials used in this study include FTO substrate (Solaronix), Ti-Nanoxide BL/SP (Solaronix), sputtering metal target TiO_2 99.99%, Ti-Nanoxide T/SP (Solaronix), Ti-Nanoxide R/SP (Solaronix), Titanium (IV) (triethanolaminato) isopropoxide solution (TTEAIP, Sigma Aldrich), acetone (Merck), ethanol (Merck, 99.8%), 2-propanol (Merck), dye N719, electrolyte (Mesolyte TDE-250, Solaronix), surlyn (Meltonix 1170-25 sealing), and test cell platinum electrodes drilled (Pt, Solaronix).

Deposition Blocking Layer Sputtering

The fabrication of TiO_2 sputtering-based blocking layer photoanodes begins with cleaning the FTO substrate using ultrasonic waves in soap solution and aquades for 15 minutes each. After that, the substrate is immersed in acetone at a temperature of 80°C. The first layer of the photoanode is the blocking layer (BL), wherein this study, the RF sputtering method is used. The sputtering process is controlled with a pressure of 9×10^{-1} Pa, a gas flow rate of 60 sccm, an air pressure control of 26%, and a substrate rotation of 5 rpm. Then dried at temperatures of 100, 300, and 500°C, respectively.

Deposition Blocking Layer Spin Coating

Samples that have been deposited with a sputtered blocking layer are coated with a colloidal blocking layer (Ti-Nanoxide BL/SP) using the spin coating method at a speed of 3000 rpm for 1 minute and dried at temperatures of 100, 300, and 500°C, respectively. Furthermore, the process of making DSSC photoanodes is like our previous work [5], as shown in Figure 1.

RESULTS AND DISCUSSION

The structural properties of the blocking layer (BL) and multilayer blocking layer TiO_2 deposited using the sputtering and spin coating methods were characterized using XRD. Figure 2 shows the XRD spectra of the BL and multilayer BL TiO_2. All the peaks observed in the spectrum correspond to the anatase phase of TiO_2 COD-9009086. As we can see in the image, there are no impurity phases or other oxides in the crystal structure, indicating pure TiO_2 [12].

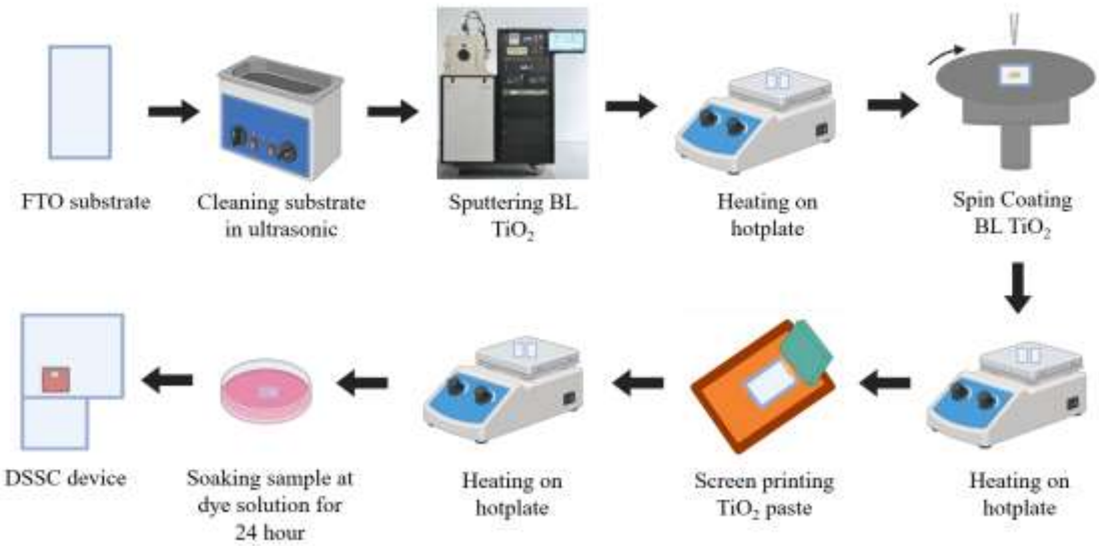

Figure 1. Deposition multilayer BL TiO_2

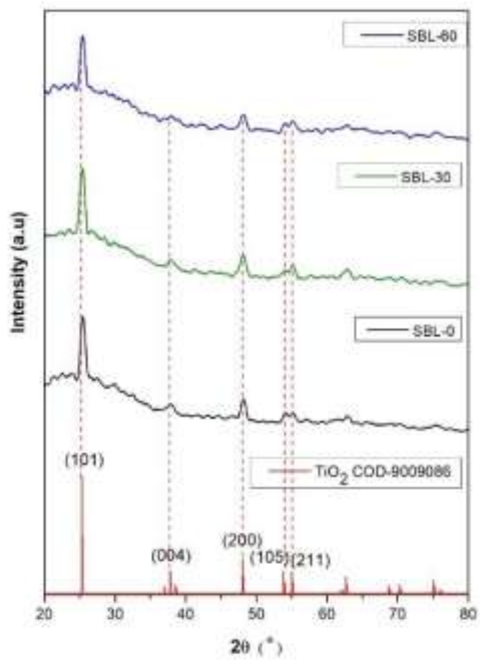

Figure 2. The XRD pattern of SBL-0, SBL-30, and SBL-60

To calculate the crystal size, the following Debye-Scherrer formula can be used [18]:

$$D = \frac{k\lambda}{\beta \cos \theta} \quad (1)$$

where λ = the wavelength of X-rays (1.54056 Å), θ = the Bragg diffraction angle, and β = full width at half maximum (FWHM) of the most dominant peak [19]. The crystal sizes for SBL-0, SBL-30, and SBL-60 are 17.24 nm, 20.69 nm, and 25.86 nm, respectively.

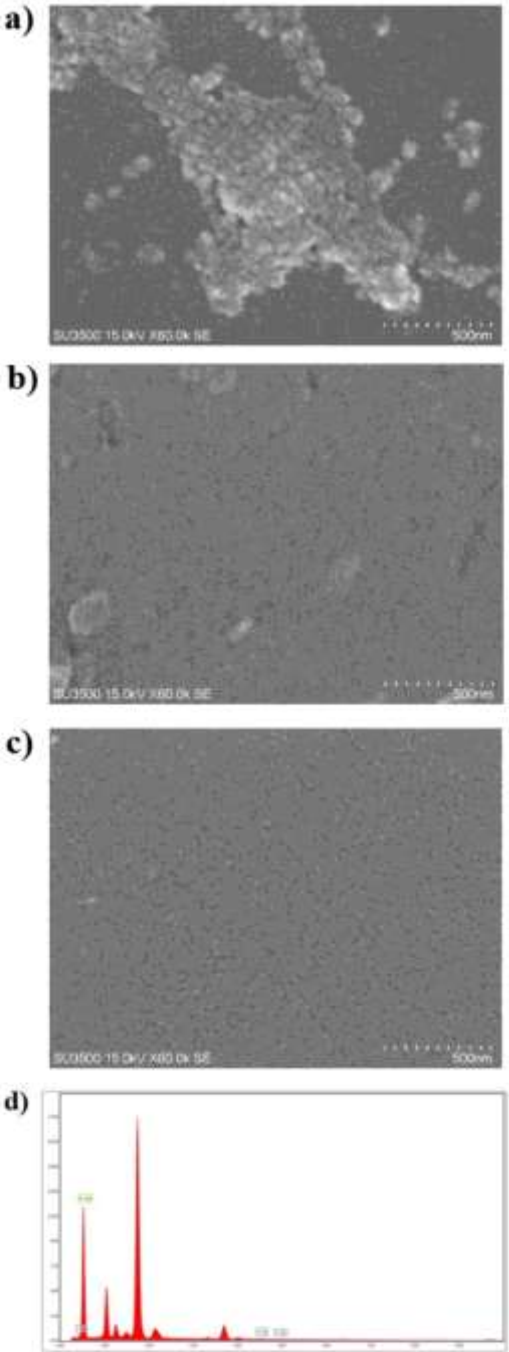

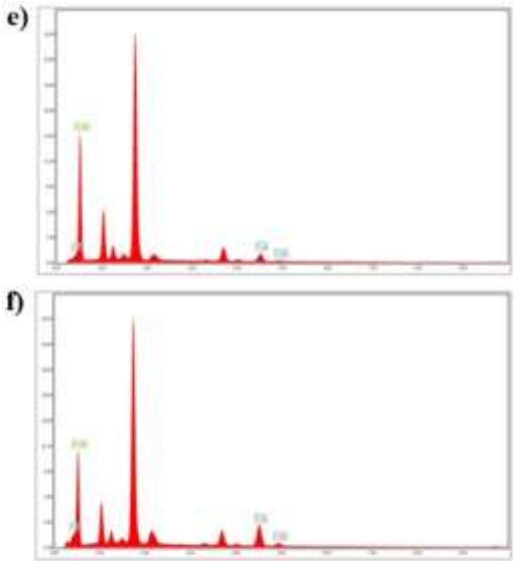

Figure 3. The SEM image of a) SBL-0, b) SBL-30, and c) SBL-60 and EDX of d) SBL-0, e) SBL-30, and f) SBL-60

The SEM surface morphology images of the compact films SBL-0, SBL-30, and SBL-60 are presented in Figure 3(a-c). All the compact films show that the FTO glass is uniformly covered with a dense TiO_2 layer, indicating good adhesion at the FTO/TiO_2 interface [20], [21]. This can act as a BL between FTO used as a transparent conductive electrode and TiO_2 to suppress electron recombination in DSSC [20].

Table 1. Porosity of multilayer BL TiO_2

Samples	Porosity (%)
SBL-0	67.69
SBL-30	65.81
SBL-60	72.83

The EDX analysis of BL SBL-0, SBL-30, and SBL-60 deposited on FTO was conducted to identify their composition. Figure 3(d-f) shows the elements Ti and O, indicating that the TiO_2 phase has formed for all samples. Additionally, a porosity of 67.69, 65.81, and 72.83% was also obtained for SBL-0, SBL-30, and SBL-60, respectively, as shown in Table 1. The multilayer TiO_2 blocking layer shows higher porosity due to the controlled deposition process, which allows for better structural integrity and reduced charge recombination [16]. High porosity in the blocking layer reduces charge recombination by creating a complex pore structure that effectively suppresses the diffusion of I_3^- ions to the FTO substrate, thereby reducing electron recombination between electrons on the substrate and I_3^- ions [22].

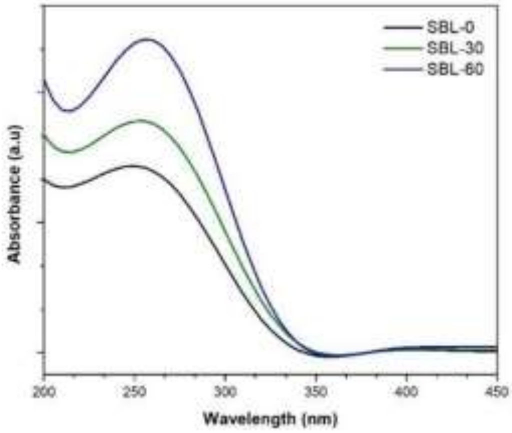

Figure 4. Absorbance spectrum SBL-0, SBL-30, and SBL-60

The measurement of optical absorption was conducted using a UV–Vis spectrometer. Figure 4 shows the absorption spectra of BL and multilayer BL TiO_2. The maximum absorption of SBL-0 is at a wavelength of 248 nm, SBL-30 at 253 nm, and SBL-60 at 257 nm. According to the UV-Vis absorption spectrum of BL and multilayer BL TiO_2, the spectral response of multilayer BL TiO_2 has a higher absorption intensity. The absorbance for the multilayer TiO_2 blocking layer is greater due to the combined effect of multiple layers, which allows for increased dye adsorption and enhanced light absorption [23]. Additionally, the absorption edge shifts to longer wavelengths for SBL-60. This is because the Fermi level will be within the conduction band since electrons occupy states below the Fermi level in the conduction band, causing the absorption edge to shift to higher energy or produce a blue shift [24].

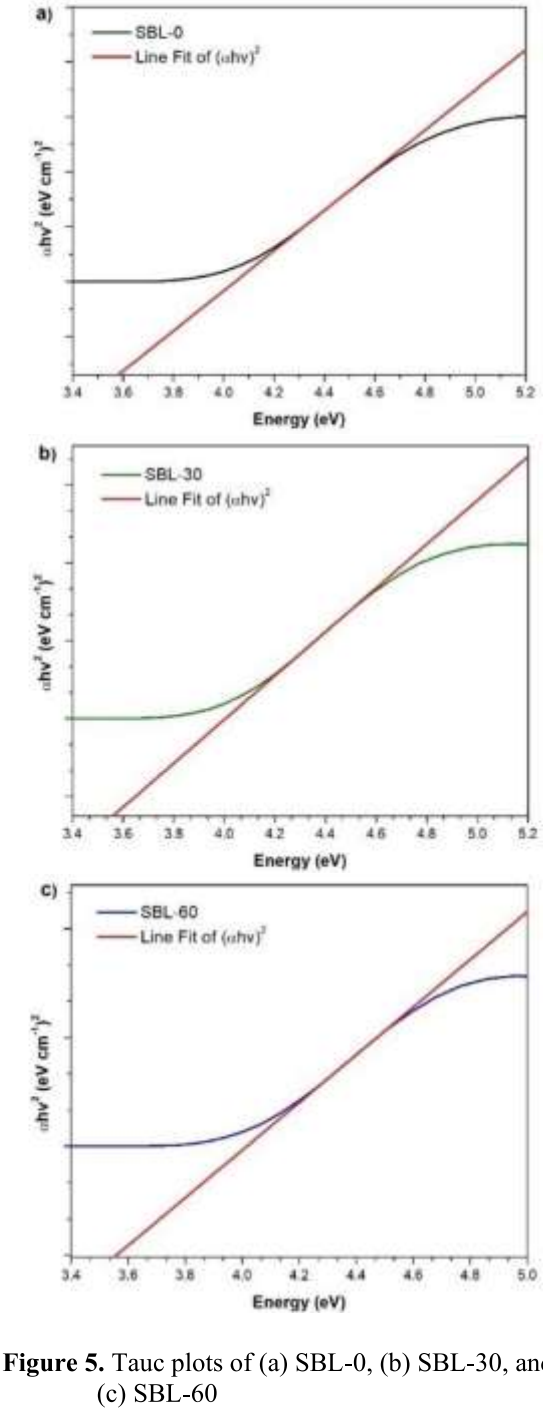

Figure 5. Tauc plots of (a) SBL-0, (b) SBL-30, and (c) SBL-60

Figure 5 shows the optical band gap (E_g) of BL and multilayer BL TiO_2, calculated using the absorption coefficient with the Tauc equation. The research results show that the multilayer BL TiO_2 narrows the optical band gap of TiO_2. The optical band gap decreases from 3.58 eV for SBL-0 to 3.56 eV for SBL-30 and 3.55 eV for SBL-60, as shown in Table 2. These results indicate that SBL-60 exhibits the narrowest band gap. The reduction of the band gap in thin films will result in increased electron transport and reduced electron recombination rates, which can enhance the efficiency of DSSC [25], [26].

Table 2. Band gap of multilayer BL TiO_2

Samples	Band Gap (eV)
SBL-0	3.58
SBL-30	3.56
SBL-60	3.55

DSSC with BL and multilayer BL TiO_2 was characterized using a solar simulator with a light source of 100 mW/cm². By plotting the J-V characteristic curve values, the efficiencies of the BL and multilayer BL TiO_2 have been determined, as shown in Figure 5.

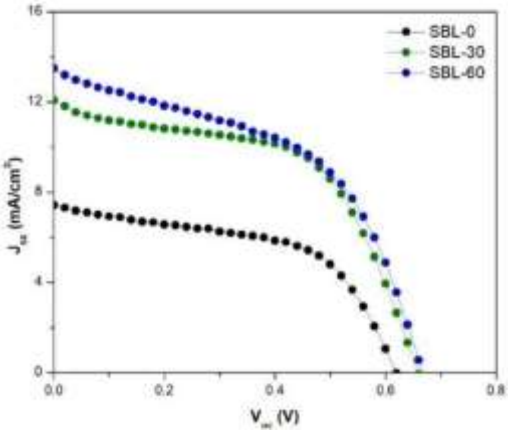

Figure 6. The J-V curves of multilayer BL TiO_2

As can be seen in Figure 6, J_{sc} and V_{oc} increased after the introduction of the double blocking layer. DSSC prepared with BL TiO_2 (SBL-0) has a lower short-circuit photocurrent density (J_{sc}) of 7.42 mA/cm² and an open-circuit voltage (V_{oc}) of 0.62 V, resulting in a low cell conversion efficiency of 2.50%. Meanwhile, the DSSC prepared with multilayer BL TiO_2 for SBL-30 and SBL-60 has higher J_{sc} values of 12.07 mA/cm² and 13.49 mA/cm², respectively, as well as higher V_{oc} values of 0.66 V and 0.67 V, respectively. Thus, a higher efficiency of 4.37% for SBL-30 and 4.49% for SBL-60 was obtained, as shown in Table 3. The increase in Jsc value is generally associated with the increase in the number of photo-generated electrons that are efficiently transferred to the TiO_2 electrode [27]. Additionally, J_{sc} increases when charge carrier recombination decreases [28]. Meanwhile, a higher V_{oc} reduces charge recombination, which ultimately results in more efficient solar energy harvesting [29]. The decreasing and diminishing electron recombination greatly enhances the efficiency of DSSC devices [30].

Table 3. The parameter performance of DSSC multilayer BL TiO_2

Samples	J_{sc} (mA/cm²)	V_{oc} (V)	FF (%)	η (%)
SBL-0	7.425	0.62	54	2.50
SBL-30	12.07	0.66	55	4.37
SBL-60	13.49	0.67	50	4.49

The dynamics of interfacial electron transport in DSSC were examined using electrochemical impedance spectroscopy (EIS) analysis. Figure 6 shows the charge transport for SBL-0, SBL-30, and SBL-60.

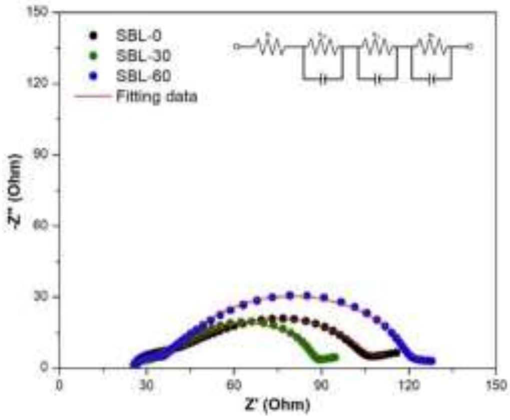

Figure 7. Nyquist plot of DSSC multilayer BL TiO_2

By using the equivalent circuit shown in the inset of Figure 7 and the Nyquist diagram installation with it, the resistance of various layers can be obtained, as shown in Table 4. As we can see, in DSSC SBL-0, an R_{ct} of about 66.41 Ω was obtained. The addition of TiO_2 BL on the FTO surface increases R_{ct}, which has made the charge transfer between FTO and TiO_2 more difficult. Therefore, by increasing R_{ct}, the current of the SBL-0 cell decreases, which is clearly visible in the J-V characteristic curve of the SBL-0 cell. Adding a multilayer BL TiO_2

reduces R_{ct} between TiO_2 nanoparticles and the FTO electrode to 53.40 Ω for SBL-30 and 12.53 Ω for SBL-60. This indicates a lower R_{ct} and results in a higher DSSC current. These results indicate a good correlation between the EIS and J-V results. In the DSSC SBL-60 cell, with the addition of a multilayer BL TiO_2, the recombination of electrons transmitted through the blocking layer decreases, resulting in better photovoltaic activity [12].

Table 4. The equivalent circuit parameter of DSSC multilayer BL TiO_2

Samples	R_s (Ω)	R_{pt} (Ω)	R_{ct} (Ω)	R_d (Ω)
SBL-0	24.68	21.17	66.41	17.29
SBL-30	24.38	6.422	53.40	12.87
SBL-60	25.00	85.83	12.53	3.906

CONCLUSIONS

The improvement in DSSC performance studied here was achieved by optimizing the structure of the TiO_2 blocking layer using sputtering and spin coating methods. The smallest band gap was obtained for SBL-60 at 3.55 eV, and this reduction in band gap can decrease the electron recombination rate in the DSSC. This is supported by the small R_{ct} obtained for SBL-60, which is 12.53 Ω. The reduction of electron recombination rate can improve the efficiency in the DSSC itself, where the best efficiency obtained in the study for SBL-60 was 4.49%.

ACKNOWLEDGEMENT

This research is supported and funded by PNBP Universitas Negeri Malang in 2024 through the thesis grant scheme.

REFERENCES

[1] Y. Ahmadi, H. Teymourinia, S. Hosseininezhad, and A. Ramazani, ‘DFT and TD-DFT optoelectronic study on hybrid alizarin-carbazol based dyes incorporated on titanium dioxide (TiO2) for dye sensitized solar cell application’, *Inorganic Chemistry Communications*, vol. 162, p. 112153, Apr. 2024, doi: 10.1016/j.inoche.2024.112153.

[2] H. Pujiarti *et al.*, ‘The Effect of Acetylene Carbon Black (ACB) Loaded on Polyacrylonitrile (PAN) Nanofiber Membrane Electrolyte for DSSC Applications’, *Micromachines*, vol. 14, no. 2, p. 394, Feb. 2023, doi: 10.3390/mi14020394.

[3] R. H. Althomali *et al.*, ‘A novel Pt-free counter electrode based on MoSe2 for cost effective dye-sensitized solar cells (DSSCs): Effect of Ni doping’, *Journal of Physics and Chemistry of Solids*, vol. 182, p. 111597, Nov. 2023, doi: 10.1016/j.jpcs.2023.111597.

[4] A. Ma’arifah, N. Sholeha, M. Nurhamidah, R. Diningsih, and H. Pujiarti, ‘The Effect of Sputtering Temperature of TiO2/ITO-PEN Photoanodes in Dye Sensitized Solar Cell’, *Jurnal Fisika dan Aplikasinya*, vol. 17, no. 1, pp. 37–47, Oct. 2024, doi: 10.18860/neu.v17i1.29404.

[5] H. Pujiarti, A. N. Ramadhani, N. H. Arimbi, M. Diantoro, A. N. Afandi, and Nasikhudin, ‘Effect of Polyacriontrile (PAN) Concentration on Characteristics and Performance of TiO2/N719/PAN-rGO for Dye-Sensitized Solar Cells’, in *Proceedings of the 2nd International Conference on Science Education and Sciences 2022 (ICSES 2022)*, vol. 8, A. Doyan, S. Hadisaputra, M. M. A. Kechik, M. R. Bilad, C.-M. Wei, and Susilawati, Eds., in Advances in Physics Research, vol. 8. , Dordrecht: Atlantis Press International BV, 2023, pp. 74–85. doi: 10.2991/978-94-6463-232-3_9.

[6] H. Pujiarti, N. Sholeha, M. Diantoro, and R. Hidayat, 'The Effect of Ti-Isopropoxide (TTIP) Treatment on The TiO2 Mesoporous Layer for DSSC Application', 2023.

[7] N. Shah *et al.*, 'A Review of Third Generation Solar Cells', *Processes*, vol. 11, no. 6, p. 1852, Jun. 2023, doi: 10.3390/pr11061852.

[8] A. Fauzi *et al.*, 'Exploring heterogenous TiO2 nanocrystals from natural ilmenite mineral extraction for energy application', *Materials Science for Energy Technologies*, vol. 7, pp. 216–227, 2024, doi: 10.1016/j.mset.2023.11.001.

[9] M. Samir, Z. Ismail, A. M. Agour, H. Nageh, and S. O. Abdellatif, 'Exploring forward scattering mechanisms in TiO2 with carbon quantum dots: Insights into photovoltaic applications', *Optical Materials*, vol. 148, p. 114922, Feb. 2024, doi: 10.1016/j.optmat.2024.114922.

[10] P. Mani, S. V. Nair, and M. Shanmugam, 'Thickness-dependent hole-blocking capability of RF-sputtered nickel oxide compact layers in dye-sensitized solar cells', *emergent mater.*, vol. 3, no. 2, pp. 117–124, Apr. 2020, doi: 10.1007/s42247-020-00094-1.

[11] A. Ma'arifah, N. Sholeha, H. Pujiarti, M. Diantoro, A. Hidayat, and Z. Osman, 'The effect of RF sputtering power variation on blocking layer TiO2 on the performance of DSSC', *Results in Surfaces and Interfaces*, vol. 18, p. 100456, Jan. 2025, doi: 10.1016/j.rsurfi.2025.100456.

[12] A. Zatirostami, 'Increasing the efficiency of TiO2-based DSSC by means of a double layer RF-sputtered thin film blocking layer', *Optik*, vol. 207, p. 164419, Apr. 2020, doi: 10.1016/j.ijleo.2020.164419.

[13] M. N. Mustafa, S. Shafie, M. H. Wahid, and Y. Sulaiman, 'Preparation of TiO2 compact layer by heat treatment of electrospun TiO2 composite for dye-sensitized solar cells', *Thin Solid Films*, vol. 693, p. 137699, Jan. 2020, doi: 10.1016/j.tsf.2019.137699.

[14] Y. Wang, W. Wu, and P. Ren, 'Classification, Functions, Development and Outlook of Photoanode Block Layer for Dye-Sensitized Solar Cells', *Inorganics*, vol. 13, no. 4, p. 103, Mar. 2025, doi: 10.3390/inorganics13040103.

[15] K. Ozel, A. Atilgan, and A. Yildiz, 'Multi-layered blocking layers for dye sensitized solar cells', *Journal of Photochemistry and Photobiology A: Chemistry*, vol. 448, p. 115297, Feb. 2024, doi: 10.1016/j.jphotochem.2023.115297.

[16] M. Sibiński, 'Impact of blocking layers based on TiO2 and ZnO prepared via direct current reactive magnetron sputtering on DSSC solar cells', *Scientific Reports*, 2024.

[17] H.-W. Kang, J.-W. Lee, and N.-G. Park, 'Effect of double blocking layers at TiO_2 /Sb_2 S_3 and Sb_2 S_3 /spiro-MeOTAD interfaces on photovoltaic performance', *Faraday Discuss.*, vol. 176, pp. 287–299, 2014, doi: 10.1039/C4FD00126E.

[18] M. Ayaz, M. Hijji, A. S. Alatawi, M. A. Namazi, and M. I. M. Ershath, 'Improving charge transfer properties and solar cell performance by In-doped TiO2 as an efficient photoanode for dye-sensitized solar cells (DSSCs)', *Journal of Physics and Chemistry of Solids*, vol. 188, p.

111913, May 2024, doi: 10.1016/j.jpcs.2024.111913.

[19] D. P. Dave and K. V. Chauhan, 'Synthesis of visible spectrum-active TiO2 thin film induced by RF magnetron sputtering', *Materials Today: Proceedings*, vol. 62, pp. 4254–4259, 2022, doi: 10.1016/j.matpr.2022.04.755.

[20] B.-R. Koo, D.-H. Oh, and H.-J. Ahn, 'Influence of Nb-doped TiO 2 blocking layers as a cascading band structure for enhanced photovoltaic properties', *Applied Surface Science*, vol. 433, pp. 27–34, Mar. 2018, doi: 10.1016/j.apsusc.2017.10.078.

[21] F. Lv *et al.*, 'N-I co-doped TiO2 compact film as a highly effective n-type electron blocking layer for solar cells', *Journal of Alloys and Compounds*, vol. 837, p. 155555, Oct. 2020, doi: 10.1016/j.jallcom.2020.155555.

[22] H.-L. Yao *et al.*, 'Nano-Porous TiO_2 Layer Using Ultrafine Nano-Particles for the Blocking Layer in Dye-Sensitized Solar Cells', *j nanosci nanotechnol*, vol. 14, no. 4, pp. 2829–2835, Apr. 2014, doi: 10.1166/jnn.2014.8602.

[23] J. Park and M. Lee, 'Performance enhancement of dye-sensitized solar cell with a TiCl4-treated TiO2 compact layer', *Electron. Mater. Lett.*, vol. 11, no. 2, pp. 271–275, Mar. 2015, doi: 10.1007/s13391-014-4130-6.

[24] G. R. Neupane, A. Kaphle, and P. Hari, 'Microwave-assisted Fe-doped ZnO nanoparticles for enhancement of silicon solar cell efficiency', *Solar Energy Materials and Solar Cells*, vol. 201, p. 110073, Oct. 2019, doi: 10.1016/j.solmat.2019.110073.

[25] G. A. Alamu, P. S. Ayanlola, O. Adedokun, Y. K. Sanusi, and G. R. Fajinmi, 'Enhanced photovoltaic performance of green synthesized Fe3O4 nanostructures embedded in TiO2 photoanode for dye sensitized solar cells', *Optik*, vol. 300, p. 171642, Apr. 2024, doi: 10.1016/j.ijleo.2024.171642.

[26] M. Irfan *et al.*, 'Modification in the efficiency of dye-sensitized solar cells (DSSCs) by H ions implantation on TiO2 photoanode', *DJNB*, vol. 20, no. 1, pp. 89–101, Jan. 2025, doi: 10.15251/DJNB.2025.201.89.

[27] C. H. Huang, K. S. Chang, and C. Y. Hsu, 'TiO2 compact layers prepared for high performance dye-sensitized solar cells', *Electrochimica Acta*, vol. 170, pp. 256–262, Jul. 2015, doi: 10.1016/j.electacta.2015.04.162.

[28] F. Kabir and S. N. Sakib, 'Various impacts of blocking layer on the cell stability in natural dye based dye-synthesized solar cell', *Optik*, vol. 180, pp. 684–690, Feb. 2019, doi: 10.1016/j.ijleo.2018.11.142.

[29] H.-L. Jia, M.-D. Zhang, W. Yan, X.-H. Ju, and H.-G. Zheng, 'Effects of structural optimization on the performance of dye-sensitized solar cells: spirobifluorene as a promising building block to enhance V_{oc}', *J. Mater. Chem. A*, vol. 4, no. 30, pp. 11782–11788, 2016, doi: 10.1039/C6TA03740B.

[30] J.-J. Huang, S.-L. Ou, C.-F. Hsu, and X.-Q. Shen, 'The effect of boric acid concentration on the TiO2 compact layer by liquid-phase deposition for dye-sensitized solar cell', *Applied Surface Science*, vol. 477, pp. 7–14, May 2019, doi: 10.1016/j.apsusc.2018.05.113.